Les Cahiers du GERAD ISSN: 0711–2440

Counterparty risk: CVA variability and value at risk

M. Breton,
O. Marzouk

G–2018–13

March 2018

La publication de ces rapports de recherche est rendue possible grâce au soutien de HEC Montréal, Polytechnique Montréal, Université McGill, Université du Québec à Montréal, ainsi que du Fonds de recherche du Québec – Nature et technologies.

Dépôt légal – Bibliothèque et Archives nationales du Québec, 2018
– Bibliothèque et Archives Canada, 2018

The publication of these research reports is made possible thanks to the support of HEC Montréal, Polytechnique Montréal, McGill University, Université du Québec à Montréal, as well as the Fonds de recherche du Québec – Nature et technologies.

Legal deposit – Bibliothèque et Archives nationales du Québec, 2018
– Library and Archives Canada, 2018

GERAD HEC Montréal
3000, chemin de la Côte-Sainte-Catherine
Montréal (Québec) Canada H3T 2A7

Tél. : 514 340-6053
Téléc. : 514 340-5665
info@gerad.ca
www.gerad.ca

Counterparty risk: CVA variability and value at risk

Michèle Breton [a]
Oussama Marzouk [b]

[a] *Department of Decision Sciences, HEC Montréal, Montréal (Québec), Canada, H3T 2A7*

[b] *Deloitte LLP, Canada*

michele.breton@hec.ca
omarzouk@deloitte.ca

March 2018
Les Cahiers du GERAD
G–2018–13

Abstract: The third installment of the Basel Accords advocates a capital charge against Credit Valuation Adjustment (CVA) variability. We propose an efficient numerical approach that allows to compute risk measures for the CVA process by assessing the distribution of the CVA at a given horizon. Numerical experiments are presented to illustrate the impact of various parameters and assumptions on the CVA distribution.

Keywords: Credit risk, credit valuation adjustment, value at risk

Résumé : À la suite de la crise financière de 2007, la réforme de Bâle III recommande, entre autres, la mise en place de frais de capital couvrant la variabilité de l'ajustement CVA pour le risque de contrepartie. Nous proposons une méthode numérique efficace permettant de calculer des mesures de risque à partir de la distribution du CVA à un horizon donné. Des illustrations numériques sont présentées afin d'illustrer l'impact, sur la distribution du CVA, de la valeur de divers paramètres ainsi que de certaines hypothèses simplificatrices utilisées en pratique.

Mots clés : Risque de crédit, CVA, valeur à risque

Acknowledgments: Research supported by NSERC (Canada). The authors thank professor Damiano Brigo for his valuable comments.

1 Introduction

Counterparty risk, defined as the risk of incurring losses in mark-to-market derivative positions at a counterparty default event, was one of the major issues underlying the financial crisis of 2007–2008. Counterparty risk is a hybrid type of risk; it can be seen as a complex combination of default and market risk. The likelihood of a counterparty default is related to the default risk, while the amount that can potentially be lost (the *exposure*) is driven by market risk and by the movements of market factors. Counterparty risk is particularly relevant in over-the-counter markets, which are not subject to the same tight regulatory requirements as exchange markets.

The Credit Value Adjustment (CVA) is the price of counterparty risk. Pricing the CVA has been advocated by regulators since the second installment of the Basel Accords (Basel Committee on Banking Supervision 2006). However, during the financial crisis, major losses were caused by movements in the CVA itself. In fact, most institutions were hit by accounting mark-to-market losses rather than real losses due to actual defaults. In more colloquial terms, the volatility of the price of counterparty risk caused much more damage than the default risk itself. As a result, the third installment of the Basel Accords (Basel Committee on Banking Supervision 2011) introduced a capital charge against CVA variability.

From a practical standpoint, determining such a capital charge implies assessing the probability distribution of CVA prices at a given future risk horizon, from which various volatility and risk measures for the CVA process can be computed, for instance the Value at Risk (CVA VaR), Tail Value at Risk (CVA TVaR) or expected shortfall.

Establishing the probability distribution of CVA prices raises both computational and conceptual issues. First, the valuation of a single CVA price is often computationally intensive. Such valuation is generally done using Monte Carlo methods, especially for exotic derivatives for which a direct computation is not possible (Cesari et al. 2009, Gregory 2010, Brigo et al. 2013). Because Monte Carlo simulation produces a single estimate for one point in space and time, sampling the probability distribution of future CVA prices at the risk horizon would require nested simulations that generally exceed standard computational capacities. In practice, nested simulation approaches use a very small number of scenarios in order to assess the distribution of the CVA, which makes the credibility of risk measures such as the CVA VaR questionable (Brigo et al. 2013). Alternatively, computations can be simplified through ad-hoc assumptions such as a constant credit exposure, which eliminates the impact of market risk on the CVA price.

Second, the CVA is by nature a pricing component, while risk measurement pertains to real-world profit and loss. Accordingly, the distribution of the CVA should be assessed under the real (historical) probability measure (denoted by $\mathbb{P}$), while the CVA price itself is obtained under the risk-neutral (or pricing) measure $\mathbb{Q}$. This consideration is often ignored in practice because the estimation of the $\mathbb{P}$-parameters is generally problematic.

In this paper, we show how the pricing approach of Breton and Marzouk (2018) can be used to obtain the distribution of the CVA at a given risk horizon. This pricing approach is based on backward induction rather than forward simulation, which makes it possible to characterize the CVA as a known function of the market risk factors in a single execution. A precise distribution of the CVA, based on a large number of possible scenarios, can then be obtained very efficiently, provided that the number of risk factors is not too high.

The contribution of the paper is twofold. First, we propose an efficient approach for the computation of capital charges against CVA variability, such as the CVA VaR, and provide illustrative examples to show the versatility and efficiency of this approach. Second, we discuss the impact of various market and risk parameters on the distribution of the CVA and on the associated risk measures. In particular, we address the issue of wrong-way risk (WWR), which is the additional risk faced when the exposure and the counterparty's default are positively correlated, and we assess the impact on risk estimate values of using the risk-neutral distribution instead of the physical distribution.

The paper is organized as follows. Section 2 sets the procedure for estimating the CVA VaR or any other risk measure based on the CVA distribution. Section 3 recalls the pricing framework and the recursive algorithm of Breton and Marzouk (2018). Section 4 reports on numerical experiments and provides various sensitivity analyses. Section 5 is a conclusion.

2 Estimating the CVA distribution

Consider a defaultable contract between an investor and a counterparty, with an inception date $t = 0$ and maturity T. We denote by $\{X_t\}_{0\leq t\leq T}$ the vector process of all relevant market- and default-risk factors; this vector process may include, for instance, the contract's underlying factors, the short interest rate, and the risk factors underlying the counterparty default process. The CVA is an adjustment applied to the value of a derivative position to account for a potential default by the counterparty. The value of this adjustment depends on the time to maturity and the anticipated evolution of the underlying market and risk factors. Assuming that the process $\{X_t\}$ is Markovian, the CVA can be expressed as a function of the current date and of the current value of the market and risk factors, and we denote by $\mathrm{CVA}_t(x)$ the value of the CVA at date t when $X_t = x$.

The CVA adjustment is computed at $t = 0$ and is marked to market at regular intervals. To assess the risk of adverse changes in the mark-to-market CVA for a given risk horizon H, one needs to evaluate, at some date $s \in [0, T - H]$ where X_s is observed, the probability distribution of the CVA at date $s + H$, or, equivalently, the probability distribution of the change in the value of the CVA in the time interval $[s, s + H]$.

One possible way of doing this is to simulate the vector process X_t over the time interval $(s, s + H]$ from the known value X_s, thereby generating a sample of values for the risk factors affecting the contract; this simulation is performed using the model dynamics of the risk factors under the real probability measure $\mathbb{P}$. The second step consists of evaluating the CVA at date $s + H$ for all simulated values of X_{s+H}, yielding a sample of possible CVA values at the risk horizon. If the sample is sufficiently large,[1] the observed CVA value frequencies give an approximation of the CVA distribution at the risk horizon, from which various risk measures can be obtained. The CVA VaR advocated in Basel III, for instance, is a quantile of the distribution of the differences between the (simulated) future values $\mathrm{CVA}_{s+H}(X_{s+H})$ and the (observed) current $\mathrm{CVA}_s(X_s)$.

Except for very simple products, pricing the CVA is a challenging task, traditionally relying on Monte Carlo simulation. The nested simulation procedure entails simulating trajectories for the default process and the market factors over the time period $(s + H, T]$, starting from each of the sample values X_{s+H}, in order to price the expected loss in each case; this simulation is performed using the model dynamics of the risk factors under the risk-neutral probability measure $\mathbb{Q}$. The nested simulation approach rapidly becomes computationally prohibitive; for instance, if a CVA price can be obtained in 60 CPU seconds, using a sample of 100,000 scenarios, the estimation of the CVA VaR, using even a small sample (say 1,000 scenarios), would require 17 hours of computing time.

It is worth noting that Basel III proposed two methods for computing the CVA VaR. The first, called the *standard* approach, is a formula that can be related to a standard variance-covariance method. This approach suffers from known shortcomings related to the use of a normal distribution and its difficulty in accommodating tail and extreme events. The second (*advanced*) approach consists of simulating, over the time period $(s, s + H]$, only the factors of X_t related to the counterparty default process, under the assumption of a constant exposure over the risk period. As discussed in Gregory (2012), the constant-exposure assumption can be justified by the fact that default risk volatility was the main source of CVA volatility during the financial crisis. However, since counterparty risk is a combination of default risk and market risk, eliminating the latter may dramatically underestimate the probability of extreme CVA losses and CVA variability. As outlined in Pykhtin (2012), neither of the two approaches accounts for the sensitivity of the CVA to underlying market-variable movements, particularly in the presence of right-way or wrong-way risk.

One important issue that arises when determining the CVA's probability distribution is estimating the dynamics of the risk factors under both $\mathbb{P}$ and $\mathbb{Q}$. The $\mathbb{Q}$ dynamics can be estimated by calibrating the models

[1] The sample size required to obtain a good approximation depends on the dimension of the random vector process and on the complexity of the associations between the various risk factors.

to the observed current derivative prices; the only assumption underlying the calibration procedure is that markets are efficient, so that all available information is embedded in the current prices. However, estimating the $\mathbb{P}$ dynamics is more challenging and generally relies on historical data; the implicit assumption underlying historical estimation is the stationarity of the risk factor dynamics. However, it is not clear how long such a stationarity assumption can hold. In practice, a trade-off must be made as regards the length of the period used for statistical inference: while stationarity is more likely to hold over short periods, the accuracy of statistical inference increases with the number of observations. In practice, the $\mathbb{P}$ vs. $\mathbb{Q}$ issue is often neglected, and both the pricing and risk measurements are performed under the same probability measure.

In the next section, we recall the pricing approaches of Brigo and Masetti (2006) and Breton and Marzouk (2018), and show how the latter can be used to obtain a precise distribution of the CVA at the risk horizon in an efficient manner. This will enable us to evaluate the impact of the simplifications that are presently used in practice, such as the assumption of constant exposure and the use of the risk-neutral measure to assess CVA variability.

3 Pricing framework

Denote by $\{Y_t\}_{0\leq t\leq T}$ the (possibly multidimensional) process of the contract's underlying factors, including the short interest rate, denoted by $\{r_t\}_{0\leq t\leq T}$. Denote by $\{\lambda_t\}_{0\leq t\leq T}$ the (possibly multidimensional) process characterizing the counterparty default risk. Let τ be the counterparty's default time. For instance, τ could represent the first jump time of an exogenous Cox process with intensity process $\{\lambda_t\}$, or the first passage of the counterparty value process $\{\lambda_t\}$ below some deterministic default barrier. The vector process of all relevant risk factors is assumed Markovian and is defined by $\{X_t\} \equiv \{Y_t, \lambda_t\}$.

Let $V_t^D(x)$ denote the value of the defaultable claim at t when $X_t = x$, and let $V_t(x)$ denote the value of a counterparty-risk-free claim with the same characteristics as the defaultable claim at t when $X_t = x$. The CVA at (t, x) is then defined by

$$\mathrm{CVA}_t(x) \equiv V_t(x) - V_t^D(x). \tag{1}$$

Brigo and Masetti (2006) show that the CVA can be computed as the expected potential loss, under the risk-neutral measure $\mathbb{Q}$, from a derivative contract due to a possible default by the counterparty at some future time. They then provide a general pricing formula for European-style contracts:

$$\mathrm{CVA}_t(x) = (1-R)\,\mathbb{E}^{\mathbb{Q}}_{t,x}[\mathbb{I}_{(t,T]}(\tau)\Gamma_t(\tau)\max\{V_\tau(X_\tau);0\}], \tag{2}$$

where

$R \in [0,1]$ is a constant recovery factor

$\mathbb{E}^{\mathbb{Q}}_{t,x}(\cdot)$ is the expectation, under the risk-neutral measure $\mathbb{Q}$, conditional on $X_t = x$

$\mathbb{I}_A(\tau)$ is the indicator function of $\tau \in A$

$\Gamma_t(\tau) = \exp\left(-\int_t^\tau r_s ds\right)$ is the discount factor between dates t and τ.

In most practical cases, the expectation in (2) cannot be computed in closed form, and Equation (2) is the foundation for the pricing approach by Monte Carlo simulation described in the preceding section. The CVA at $(s, X_s = x)$ is evaluated by averaging the losses due to counterparty default on a sample of trajectories $(X_t)_{s\leq t\leq T}$ emanating from x.

Breton and Marzouk (2018) propose a different pricing approach, which is based on a recursive characterization. Consider a set $\mathcal{T} = \{t_m, m = 0, ..., M\}$ of discrete dates where the CVA is to be evaluated, with $t_M = T$. For European-style contracts, they show that the CVA satisfies

$$\begin{aligned} \mathrm{CVA}_{t_m}(x) &= B_m(x) + \mathbb{E}^{\mathbb{Q}}_{t_m,x}\left[\alpha_m \mathrm{CVA}_{t_{m+1}}\left(X_{t_{m+1}}\right)\right] && (3)\\ \mathrm{CVA}_T(x) &= 0 && (4)\end{aligned}$$

where $B_m(x)$ is the expected loss between t_m and t_{m+1} and $\alpha_m = \mathbb{I}_{(t_{m+1},T]}(\tau)\Gamma_{t_m}(t_{m+1})$. Their formula applies to exotic derivatives with path-dependent and/or stopping features, and to general recovery functions that can accommodate many counterparty risk mitigation techniques, such as collateral posting and netting agreements. In addition, they show how to apply a similar recursive characterization to compute the CVA of derivatives with early exercise opportunities, in a way that accounts for the change in the exercise policy due to counterparty risk.

The advantage of a recursive formulation is that it naturally leads to a dynamic programming algorithm that provides the CVA as a function of the state vector x for all evaluation dates. Typically, solving the dynamic program (3)–(4) involves computing $\mathrm{CVA}_{t_m}(\cdot)$ on a finite grid of possible values of the state vector x, and then using an interpolation scheme to obtain an analytical function $\widehat{\mathrm{CVA}}_{t_m}(\cdot)$ approximating the CVA at t_m for $x \in \mathbb{R}^n$, where n is the dimension of the state vector.

More precisely, assume that the joint density of $\left(\alpha_m, X_{t_{m+1}}\right)$ under the risk-neutral measure, conditional on $X_{t_m} = x$, is known, and suppose that $\mathrm{CVA}_{t_{m+1}}(\cdot)$ is known analytically on $\mathbb{R}^n$. Let $\mathcal{G}^n \subset \mathbb{R}^n$ denote a finite set of possible values of the state vector. At a given $x \in G^n$, since both the joint density and the function $\mathrm{CVA}_{t_{m+1}}(\cdot)$ are analytical, the computation of $\mathbb{E}^{\mathbb{Q}}_{t_m,x}\left[\alpha_m \mathrm{CVA}_{t_{m+1}}\left(X_{t_{m+1}}\right)\right]$ amounts to evaluating the integral of an analytically known function. If $B_m(x)$ can be computed or approximated efficiently, (3) yields $\mathrm{CVA}_{t_m}(x)$. The interpolation of $\mathrm{CVA}_{t_m}(x)$ for $x \in G^n$ yields the interpolation function $\widehat{\mathrm{CVA}}_{t_m}$ approximating CVA_{t_m} for all possible values of the state vector. Starting from the known function $\mathrm{CVA}_T(x) = 0$, this process yields, by backward induction, analytical interpolation functions $\widehat{\mathrm{CVA}}_{t_m}$ for all evaluation dates $t_m \in \mathcal{T}$.

Breton and Marzouk (2018) use a spectral interpolation scheme that leads to a polynomial representation of the functions CVA_{t_m}. The recursive approach to CVA valuation yields M polynomial functions of degree p, where p is the number of grid points in each dimension of the state vector. These functions can be used to evaluate the CVA at any date $t_m \in \mathcal{T}$ and for any possible value of the market factors and of the hazard rate. The functions are completely characterized by a set of $\binom{n+p}{n}$ coefficients. Numerical experiments show the efficiency of the dynamic programming approach with respect to simulation methods; for low-dimensional state space, the dynamic programming approach yields the CVA at all evaluation dates and for all possible values of the state variable, in less time than is required to obtain a single estimate using a simulation procedure.

Clearly, the advantage of the recursive characterization of the CVA becomes even more significant when estimating the distribution of the CVA at some risk horizon H, as proposed in the following algorithm.

Algorithm 1

1. Let $\mathcal{T}$ include all dates s and $s+H$, where s is a date at which the CVA distribution is to be evaluated. Run the dynamic programming algorithm (3)–(4) and obtain the function $\mathrm{CVA}_t(x)$, $x \in \mathbb{R}^n$, for all $t \in \mathcal{T}$.
2. At some date $s \in \mathcal{T}$, observe the current value of the risk factors X_s. Simulate the vector process X_t over the time interval $(s, s+H]$ from the known value X_s under the real probability measure $\mathbb{P}$.
3. For each simulated value of X_{s+H}, use the known function $\mathrm{CVA}_{s+H}(x)$ to produce a sample of possible CVA values at the risk horizon or a sample of possible CVA changes by subtracting the constant $\mathrm{CVA}_s(X_s)$.
4. Various risk measures can be computed from the frequency distribution of these samples. For instance, the CVA VaR is a quantile of the frequency distribution of the sampled CVA changes.

In the next section, we present illustrative numerical experiments in which we apply Algorithm 1 to estimate the CVA VaR.

4 Numerical experiments

We now illustrate the use of the suggested methodology for the computation of the CVA VaR using two examples where Equation (2) cannot be solved in closed form: Bermudan options and interest-rate swaps, with a stochastic default risk process. In both cases, nested simulation is not a practical alternative, while the recursive characterization provides the CVA VaR in less than three minutes on a personal computer (100,000 trajectories).[2] In the case of Bermudan options, we analyze the nonlinear behavior of the CVA VaR

[2] All experiments were done using an AMD A6-6310 APU processor with 1.8 GHz of power and 8 GB of RAM.

that arises due to the nature of the CVA function, and we link these effects to the CVA sensitivities (the CVA Greeks). We also use these experiments to show that the constant-exposure assumption can greatly underestimate the CVA VaR and to examine the extent to which a distortion between $\mathbb{P}$ and $\mathbb{Q}$ can affect the results. In the case of interest-rate swaps, we investigate the impact of right-way/wrong-way risk on the CVA and its distribution.

4.1 Independent CVA of a Bermudan option

We consider monthly exercisable put options with a strike price K and various maturities and moneyness. Assume that the underlying asset price S_t follows a geometric Brownian motion and that the counterparty hazard rate λ_t follows an independent CIR process. Under the risk-neutral probability measure $\mathbb{Q}$, the dynamics of S_t and λ_t are given by

$$\begin{aligned} dS_t &= rS_t dt + \sigma S_t dW_{1t}^{\mathbb{Q}}, \\ d\lambda_t &= \xi(\theta - \lambda_t)dt + \nu\sqrt{\lambda_t}dW_{2t}^{Q}, \end{aligned}$$

where $W_{1t}^{\mathbb{Q}}$ and $W_{2t}^{\mathbb{Q}}$ are two independent Brownian motions under $\mathbb{Q}$, r is the risk-free interest rate (assumed constant), σ is the underlying asset volatility, θ is the long-run mean of the counterparty hazard rate, ξ is the speed of adjustment to the long-run mean and ν is the hazard-rate volatility. Because switching from the risk-neutral measure $\mathbb{Q}$ to the physical probability measure $\mathbb{P}$ affects the drifts of the underlying processes but not their volatility components (Girsanov's theorem), we also assume that the dynamics of S_t and λ_t under $\mathbb{P}$ are given by

$$\begin{aligned} dS_t &= \mu S_t dt + \sigma S_t dW_{1t}^{\mathbb{P}}, \\ d\lambda_t &= \xi^{\mathbb{P}}(\theta^{\mathbb{P}} - \lambda_t)dt + \nu\sqrt{\lambda_t}dW_{2t}^{\mathbb{P}}, \end{aligned}$$

where $W_{1t}^{\mathbb{P}}$ and $W_{2t}^{\mathbb{P}}$ are two independent Brownian motions under $\mathbb{P}$, μ is the rate of return of the underlying asset, $\theta^{\mathbb{P}}$ is the long-run mean of λ_t and $\xi^{\mathbb{P}}$ is the speed of adjustment to the long-run mean.

The benchmark values of the parameters are reported in Table 1. For these parameter values, Figure 1 plots the CVA at a given t of a Bermudan put option with a remaining maturity of two years, as a function of S_t/K and λ_t. This figure shows that, while the CVA function is generally increasing with the hazard rate, the relationship with exposure is not monotone, mainly due to the early-exercise feature.

Table 1: Benchmark values for Bermudan put options.

r, μ	0.05
σ	0.2
$\lambda_0, \theta, \theta^{\mathbb{P}}$	0.1
$\xi, \xi^{\mathbb{P}}$	1
ν	0.1

Table 2 reports at date $t = 0$ the current CVA and the CVA VaR at the 99% level, over risk horizons of 10 days and 1 month, for different maturities T and moneyness, for a null recovery value.

Table 2: Current CVA and 99% CVA VaR, over horizons of 10 days and 1 month, for Bermudan put options. Parameter values are given in Table 1.

	In-the-money – $S_0/K = 0.5$			At-the-money – $S_0/K = 1$			Out-of-the-money – $S_0/K = 1.5$		
T	Current	10 days	1 month	Current	10 days	1 month	Current	10 days	1 month
2	0.2058	0.0294	0.0508	0.3429	0.0418	0.0430	0.0386	0.0303	0.0539
3	0.2058	0.0294	0.0508	0.5042	0.0421	0.0488	0.1006	0.0541	0.0952
4	0.2058	0.0294	0.0508	0.6443	0.0395	0.0484	0.1762	0.0738	0.1289
5	0.2058	0.0294	0.0508	0.7659	0.0377	0.0479	0.2559	0.0892	0.1551

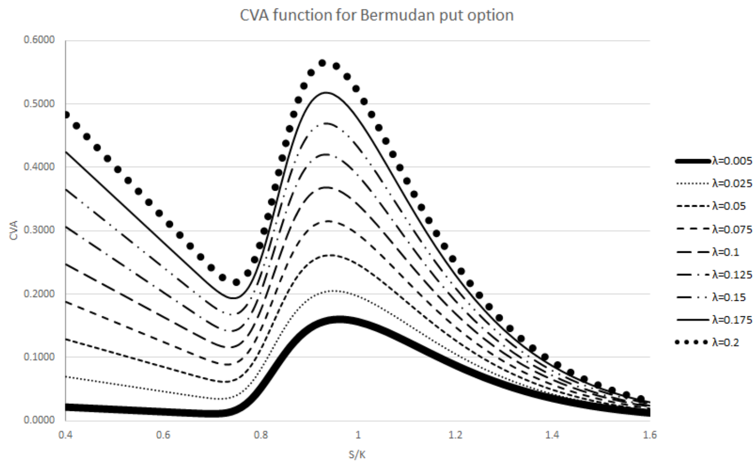

Figure 1: CVA of a Bermudan option with a maturity of 2 years and a null recovery value, as a function of hazard rate and moneyness. Parameter values are given in Table 1.

4.1.1 Impact of maturity and moneyness

Figure 2 compares the distributions of the variations in the CVA of the Bermudan option over a 10-day risk horizon and for various maturities and moneyness. For in-the-money options, we observe that the distribution and the corresponding CVA VaR estimate are not affected by their maturity. This is clearly an early-exercise effect: in-the-money, vulnerable options will be exercised early, regardless of their maturity, so that counterparty risk concerns a short time period in the near future. This is not the case for out-of-the-money options, where we can observe that the variability of the CVA and CVA VaR increase with maturity. This effect can be related to the shape of the CVA function: the slope of the option exposure in the out-of-the-money region increases with maturity, which enhances the sensitivity of the CVA to the underlying asset movements.

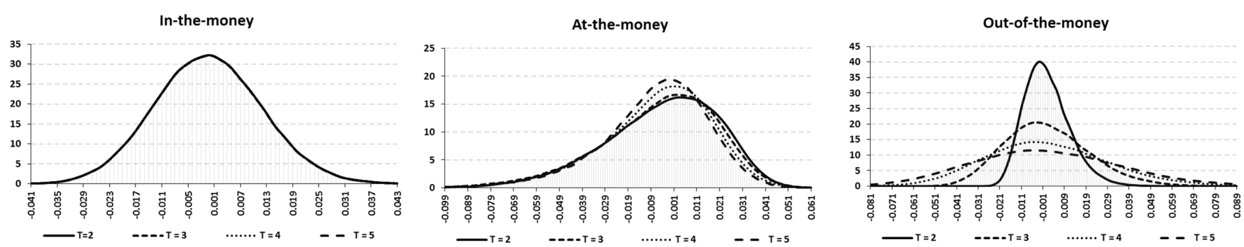

Figure 2: Impact of maturity and moneyness on the CVA distribution of a Bermudan option. Parameter values are given in Table 1.

4.1.2 Constant-exposure assumption

A common practice in the industry is to assume a constant exposure over the risk period in order to avoid nested simulations. Under a constant-exposure assumption, Equation (2) reduces to

$$\mathrm{CVA}_t(x) = (1-R)\max\left\{V_t\left(x\right);0\right\}\mathbb{E}^{\mathbb{Q}}_{t,x}[\mathbb{I}_{(t,T]}(\tau)\Gamma_t(\tau)],$$

so that changes in the CVA during the risk horizon are only related to the movements of the hazard rate.[3] In order to assess the impact of making a constant-exposure assumption on the CVA distribution, Table 3 reports the underestimation of the CVA VaR at the 99% level, due to the constant-exposure assumption, for the same instances as those reported in Table 2. This experiment shows that the constant-exposure assumption

[3] Note that, in practice, the constant-exposure assumption is not used to compute the current CVA; it is only used to compute the CVA during the risk horizon.

results in a significantly lower estimate of the CVA VaR. This effect increases with the moneyness ratio S_0/K and is particularly strong for out-of-the-money options, for which, for our benchmark parameter values, the CVA VaR can be underestimated by more than 90% under a constant-exposure assumption.

Figure 3 illustrates the impact of the constant-exposure assumption on the probability distribution of the CVA variation over a 10-day risk horizon, and shows that this assumption significantly affects the tail of the distribution of CVA movements. Figure 3 shows the impact on a five-year maturity option; the impact is similar for different maturities.

Table 3: Underestimation of the 99% CVA VaR over horizons of 10 days and 1 month for Bermudan put options under the constant-exposure assumption. Parameter values are given in Table 1.

	$S_0/K = 0.5$		$S_0/K = 1$		$S_0/K = 1.5$	
T	10 days	1 month	10 days	1 month	10 days	1 month
2	17.3%	17.7%	45.9%	46.7%	93.1%	93.3%
3	17.3%	17.7%	32.1%	26.6%	92.1%	92.3%
4	17.3%	17.7%	20.3%	11.6%	91.7%	91.9%
5	17.3%	17.7%	12.2%	2.1%	91.6%	91.7%

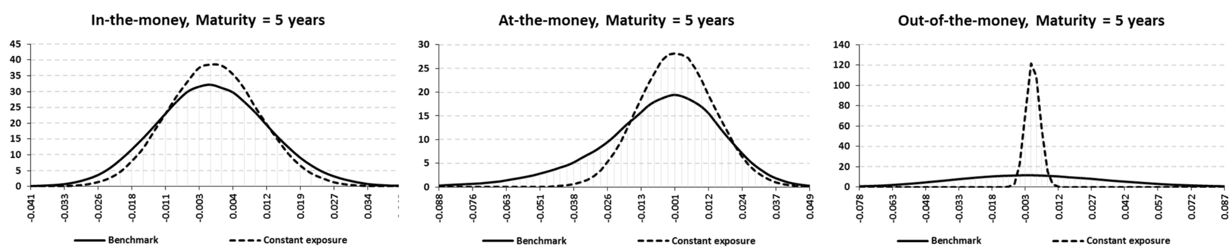

Figure 3: Impact of the constant-exposure assumption on the CVA distribution of a Bermudan option with a 5-year maturity. Parameter values are given in Table 1.

4.1.3 Model parameters

In this section, we analyze the sensitivity of the CVA VaR to various model parameters, namely, the current estimation and the volatility of the counterparty hazard rate, and the volatility of the underlying asset price. Tables 7, 8 and 9 in the Appendix compare the results reported in Table 2 (benchmark case) with those obtained by varying λ_0, ν and σ, respectively, around their benchmark values, and Figures 4, 5 and 6 compare the resulting probability distributions of the variation of the CVA over a risk horizon of 10 days for maturities of two and five years.

Figure 4 illustrates the impact of a change in the current hazard rate, where $\lambda_0 \in \{0.05, 0.1, 0.15\}$. We observe that higher values of λ_0 make the tail of the distribution heavier, and thus increase the CVA VaR estimates (this is true for all maturities and moneyness). This can be explained by two effects. The first is related to the nature of the CIR model for the hazard rate, where the volatility of the hazard-rate process is proportional to the square root of the current level of the hazard rate. Hence, higher values of λ_0 are more likely to lead to higher movements of the hazard rate in the short term, which naturally results in more pronounced CVA movements. The second effect is related to the CVA function itself; given that the CVA can be approximately assimilated to the product of the contract exposure by the default probability, the sensitivity of the CVA to the underlying asset price movements increases with the level of the hazard rate.[4] Mathematically, this effect is related to the Greek $\dfrac{\partial \mathrm{CVA}_t(x)}{\partial S_t}$. The evaluation of this partial derivative at a given $t \in \mathcal{T}$ is straightforward, given that the interpolation function $\widehat{\mathrm{CVA}}_t(x)$ is a polynomial. Observation of Figure 1 shows that the sensitivity of the CVA to changes in the underlying asset price generally increases with λ_0. Values for various hazard rates and moneyness are reported in Table 4.

[4]Note that this behavior cannot be captured under a constant-exposure assumption, where changes in the CVA are independent from changes in the underlying asset price.

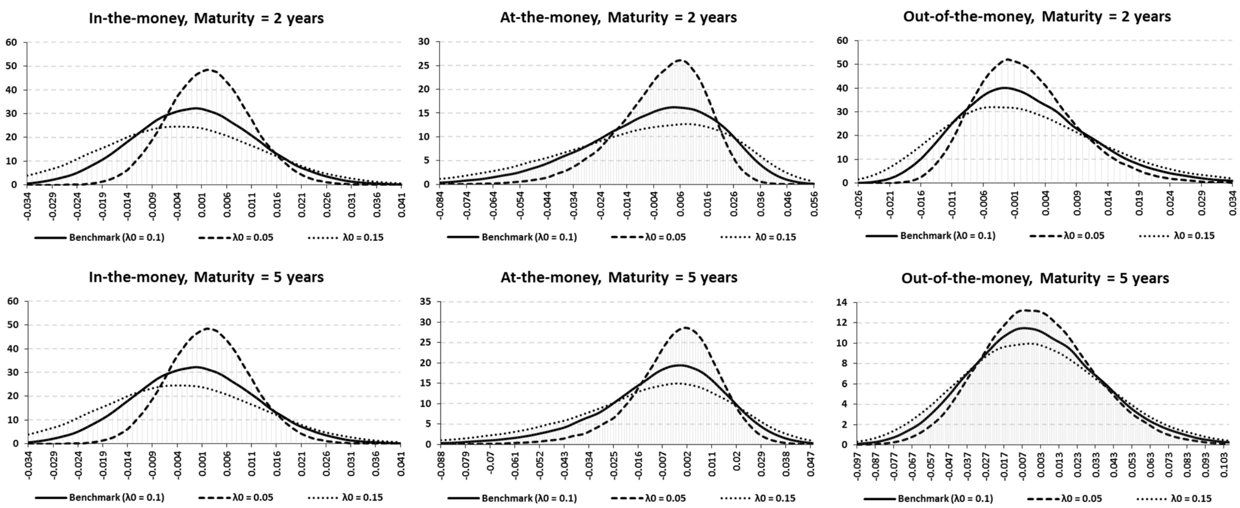

Figure 4: Impact of a change in the current hazard rate on the CVA distribution of a Bermudan option. Parameter values are given in Table 1.

Table 4: Sensivity of the CVA function to changes in price of the underlying asset, $\partial \mathrm{CVA}_t(x)/\partial S_t$, at $t = 0$ and S_0 for various values of λ_0; maturity is 2 years. Other parameters values are given in Table 1.

λ_0	$S_0/K = 0.5$	$S_0/K = 1$	$S_0/K = 1.5$
0.05	-0.0043	-0.0089	-0.0031
0.1	-0.0083	-0.0144	-0.0041
0.15	-0.0123	-0.0192	-0.0051

Figure 5 illustrates the impact of changes in the hazard-rate volatility, where $\nu \in \{0.1, 0.2, 0.3\}$. Higher values of ν result in heavier tails of the distribution of CVA changes and in higher values for the CVA VaR. This effect is more pronounced for in-the-money and at-the-money options. This is because the exposure level in these regions of the state space is relatively high, which enhances the impact of hazard-rate volatility. This effect is related to the Greek $\dfrac{\partial \mathrm{CVA}_t(x)}{\partial \lambda_t}$, which increases with the exposure level, as can be observed in Figure 1 (see also Table 5). For out-of-the-money options, the impact of the hazard-rate volatility is negligible due to a relatively low exposure level.

Table 5: Sensivity of the CVA function to changes in the hazard rate, $\partial \mathrm{CVA}_t(x)/\partial \lambda_0$, at $t = 0$, for various values of moneyness; maturity is 2 years. Parameter values are given in Table 1.

$S_0/K = 0.5$	$S_0/K = 1$	$S_0/K = 1.5$
1.9657	1.8640	0.1722

Figure 6 illustrates the impact of changes in the volatility of the underlying asset price, where $\sigma \in \{0.2, 0.25, 0.3\}$. As expected, a higher asset-price volatility increases the likelihood of significant movements in the exposure profile, thereby producing heavier tails for the distribution of the CVA movements. This effect is considerable for at-the-money and out-of-the-money options. It is relatively small for in-the-money options because of the likelihood of early exercise. Intuitively, because in-the-money options are expected to be exercised in the near future, market risk is less relevant than default risk in the short term. This is why the CVA VaR of in-the-money options is more sensitive to volatility in the hazard rate than in the underlying asset.

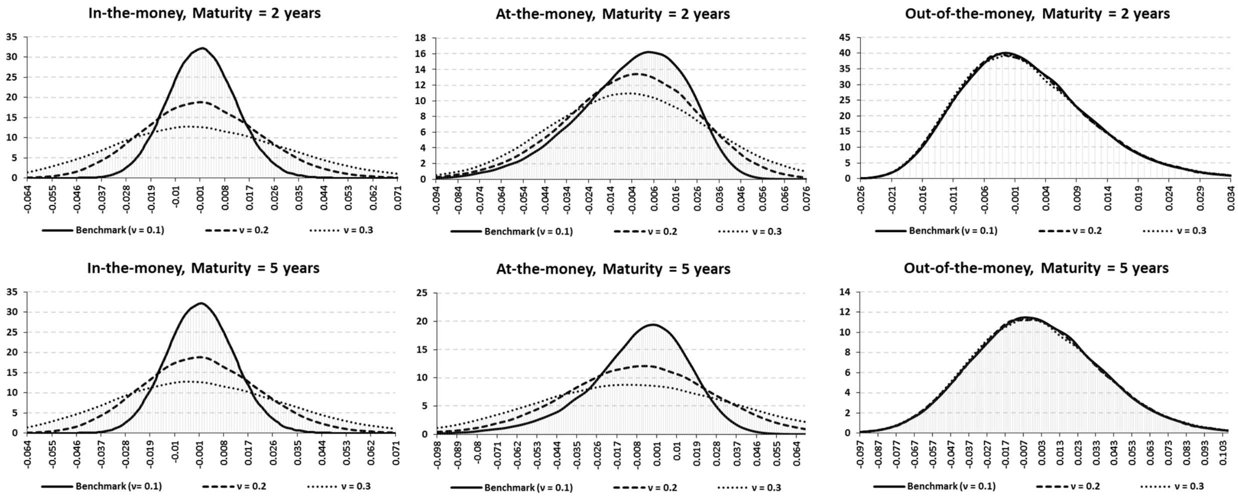

Figure 5: Impact of a change in the volatility of the hazard rate on the CVA distribution of a Bermudan option. Parameter values are given in Table 1.

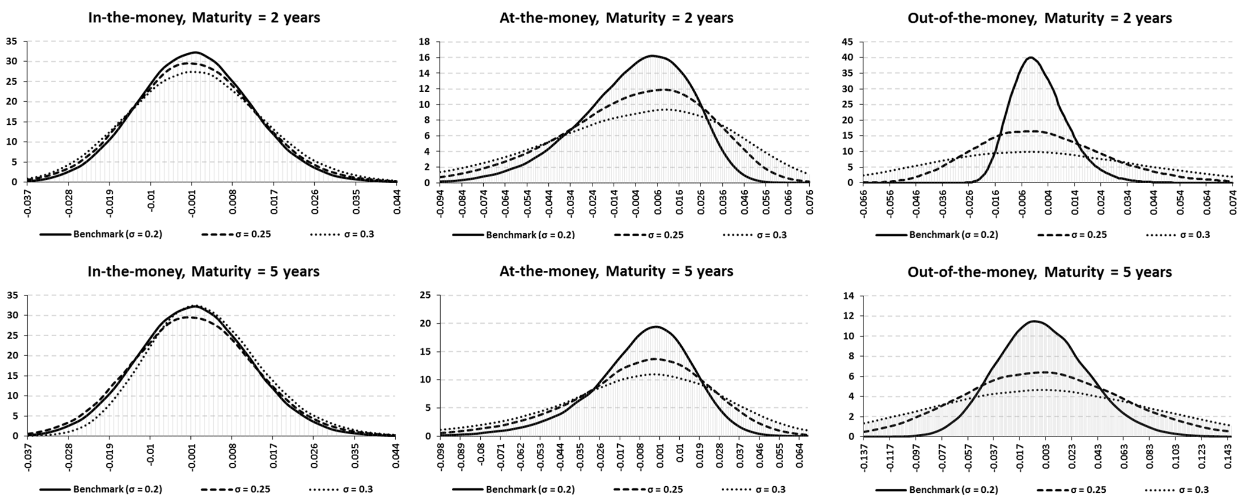

Figure 6: Impact of a change in the volatility of the hazard rate on the CVA distribution of a Bermudan option. Parameter values are given in Table 1.

4.1.4 Probability measure

Our benchmark case sets the parameters under the risk-neutral and physical probability measures to the same values. We now examine the impact of distortion between the measures $\mathbb{P}$ and $\mathbb{Q}$ on the distribution of the CVA and on the CVA VaR, by varying the values of μ, $\theta^{\mathbb{P}}$ and $\xi^{\mathbb{P}}$. Results are presented in Tables 10 to 12 in the Appendix. Recall that modifying the physical probability measure $\mathbb{P}$ has no impact on the CVA pricing function, and consequently, on the current CVA, but does result in a different sample of the risk and market factors at the risk horizon.

Comparing the benchmark results where $\mu = r = 0.05$ to results obtained for $\mu \in \{0.075, 0.1\}$ shows that changes in the value of μ have practically no impact on the distribution of the CVA, and that this is true for all maturities and moneyness. CVA VaR results are provided in Table 10.

Table 11 and Figure 7 compare the benchmark results for which $\theta^{\mathbb{P}} = \theta^{\mathbb{Q}} = 0.1$ to cases associated with $\theta^{\mathbb{P}} = 0.05$ and $\theta^{\mathbb{P}} = 0.15$. While the position of the distribution may be translated as a consequence of the mean effect resulting from changing the long-run mean of the hazard rate, the dispersion of the distribution and the CVA VaR are not significantly affected. This holds for all maturities and moneyness.

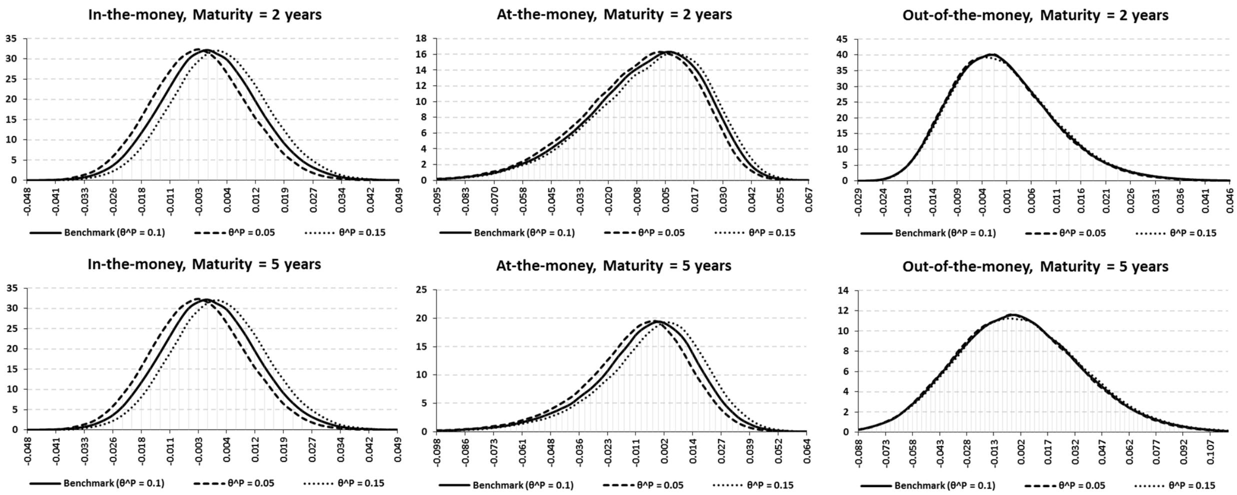

Figure 7: Distortion between the physical and risk-neutral distributions: Impact of a difference in the long-run mean of the hazard rate on the distribution of the CVA movements for a Bermudan option. Parameter values are given in Table 1.

Finally, we observe that varying $\xi^{\mathbb{P}} \in \{0.25, 1, 1.75\}$ has no significant impact on the distribution of the CVA, for all maturities and moneyness. CVA VaR results are provided in Table 12.

In summary, we observe that a distortion between the risk-neutral measure and the physical measure does not seem to significantly affect the tail of the distribution and the estimation of the CVA VaR, at least in the particular case of Bermudan options. Because the horizon for which the CVA VaR is computed is short, as is the practice for standard market VaR, the role of the drift terms in generating extreme values of the risk factors is not expected to be significant in comparison to the role of the volatility components. As discussed in Gregory (2012), drift terms become important when dealing with risk measures associated with relatively long risk horizons, such as the potential future exposure for credit limits concerns.

4.1.5 Conclusions from the Bermudan option experiment

To conclude, the behaviour of the CVA VaR can be complex due to the nonlinearity of the CVA function and the exotic characteristics of some financial contracts, for instance early-exercise opportunities. Moreover, the distributional properties of the default and market-risk factors can be relevant. The $\mathbb{P}$ vs. $\mathbb{Q}$ problem does not seem to be an important issue from a quantitative point of view, since the discrepancy between the two measures is driven by drift terms that are of secondary importance when dealing with short-horizon risk measures.

Finally, as shown in our numerical illustrations, assuming a constant exposure over the risk period can lead to significant errors. The aim of this type of simplifying assumption, which is often used in practice, is to avoid the computational burden associated with nested simulations. Note that the approach suggested in this paper is an alternative efficient computational methodology that captures all the properties of the CVA VaR without making any simplifying assumptions.

4.2 Right-way/wrong-way CVA of interest-rate swaps

We now consider payer interest-rate swap positions where fixed and floating payments are exchanged monthly. Assume that, under $\mathbb{P}$ and $\mathbb{Q}$, the spot interest rate r_t and the counterparty hazard rate λ_t follow CIR processes

$$\begin{aligned} dr_t &= \xi_r(\theta_r - r_t)dt + \nu_r\sqrt{r_t}dW_{1t} \\ d\lambda_t &= \xi_\lambda(\theta_\lambda - \lambda_t)dt + \nu_\lambda\sqrt{\lambda_t}dW_{2t}, \end{aligned}$$

where W_{1t} and W_{2t} are two correlated Brownian motions with a correlation coefficient ρ

$$dW_{1t}dW_{2t} = \rho dt.$$

In this particular case, wrong-way risk *(respectively right-way risk)* is present when $\rho > 0$ *(respectively when* $\rho < 0$*).* Since the value of a payer swap is an increasing function of the spot interest rate, when $\rho > 0$, an increase in the interest rate increases the value of the payer position, but also the likelihood of a counterparty default.

The benchmark values for the model parameters are given in Table 6. The recovery value is assumed to be null. For these benchmark parameters and a fixed payment of 5%, Figure 8 plots the CVA of a payer swap position with a remaining maturity of two years at a given date t, as a function of the spot interest rate r_t and of the hazard rate λ_t. One can observe from Figure 8 that, contrary to the Bermudan option case, the CVA function is monotone increasing in both r_t and λ_t.

Table 6: Benchmark values for the model parameters, interest-rate swaps.

r_0, θ_r	0.05
ξ_r	0.5
$\lambda_0, \theta_\lambda$	0.1
ξ_λ	1
ν_r, ν_λ	0.1

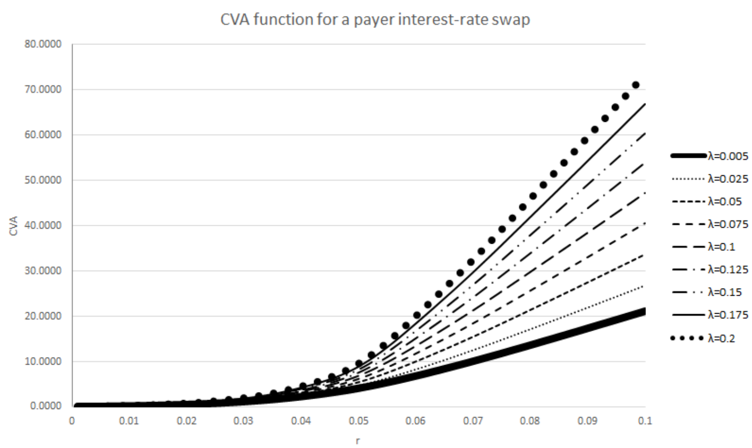

Figure 8: CVA of a payer interest-rate swap with a maturity of 2 years and a null recovery value, as a function of hazard rate and interest rate. Parameter values are given in Table 6.

In order to investigate the impact of wrong-way (respectively right-way) risk, we compute the current CVA and the CVA VaR at the 99 % level, for risk horizons of 10 days and 1 month, for various swap maturities ($T = 2, 3, 4, 5$), correlation coefficients ($\rho \in \{-0.5, 0, 0.5\}$) and hazard-rate volatility ($\nu_\lambda \in \{0.1, 0.2, 0.3\}$), where the fixed payment is chosen so as to make the swap value null at inception. Table 13 in the Appendix reports the various CVA and CVA VaR values, in basis points, obtained from these experiments.

The results show that wrong-way risk (respectively right-way risk) increases (respectively decreases) the CVA VaR estimate, for all considered maturities, even if the impact is relatively small. When the correlation is positive, scenarios in which the swap exposure is high imply higher levels of the hazard rate (as compared to the zero-correlation case), which results in more pronounced upward movements of the CVA. The reverse effect happens in the case of right-way risk. Figure 9 compares the distributions of the 10-day CVA movements implied by the three correlation levels for maturities of two and five years.

Figure 10 illustrates the role of the hazard-rate volatility in the right-way/wrong-way effect. We observe that the hazard-rate volatility enhances both the right-way and the wrong-way effects. In particular, when the correlation is negative, a higher hazard-rate volatility results in a lower CVA VaR estimate. At first glance,

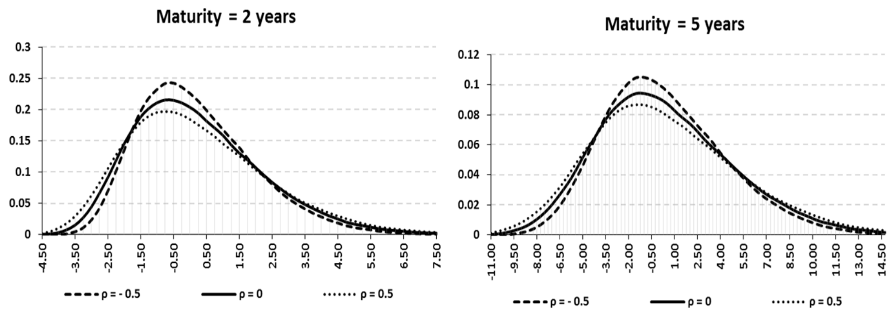

Figure 9: Impact of WWR and RWR on the CVA distribution of a payer interest-rate-swap position, at a 10-day risk horizon. Parameter values are given in Table 6.

this could seem counterintuitive, since increased volatility should lead to an increased likelihood of extreme upward movements of the CVA. However, it is important to note that the CVA is essentially driven by the contract's exposure: high-exposure scenarios are those that contribute most to the tail of the distribution, independently of hazard-rate levels. In the presence of a negative correlation, a higher hazard-rate volatility leads to lower hazard-rate levels in high-exposure scenarios, which decreases the CVA VaR estimate. The reverse effect happens in the case of wrong-way risk, resulting in a higher CVA VaR.

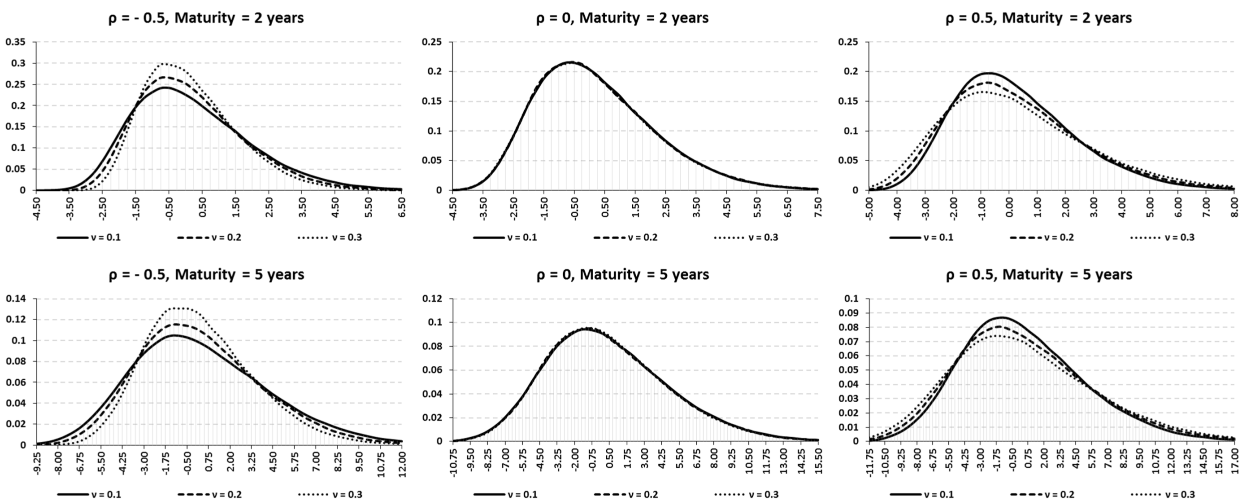

Figure 10: Impact of the hazard-rate volatility ν_λ on the wrong-way and right-way effect on the CVA distribution of a payer interest-rate swap position, at a 10-day risk horizon. Parameter values are given in Table 6.

Note that this right-way effect is not observed in the case of a higher interest-rate volatility, since the interest-rate volatility affects the exposure profile. An increased interest-rate volatility therefore increases the CVA VaR, regardless of whether the correlation is positive or negative. The asymmetric roles of the interest-rate volatility and hazard-rate volatility result from the complementary status of the exposure and the default probability: the default probability defines the likelihood of a market loss, while the exposure measures the severity of a loss if it occurs.

In summary, our results show that right-way/wrong-way risk affects not only the CVA level, but also the CVA VaR, while the hazard-rate volatility increases both the right-way and the wrong-way effects. In particular, when there is right-way risk, a higher hazard-rate volatility decreases the CVA VaR.

5 Conclusion

This paper proposes an efficient method to obtain the distribution of the CVA at a given risk horizon, from which risk measures such as the CVA VaR can be computed. This method is based on the recursive formulation of the CVA proposed in Breton and Marzouk (2018). An interesting property of this recursive pricing approach is that it yields, in a single execution, a CVA function that can be used at different dates and for different horizons, typically in less time than it takes to produce a single CVA estimate via classical Monte Carlo pricing. This makes it possible to build a robust methodology for estimating the CVA VaR and overcoming the computational issue associated with nested simulations, yielding precise estimates in a reasonable amount of time.

We provide two application examples to illustrate the use of this methodology and the kind of results that can be obtained. In light of these examples, we analyze the complex behavior of the CVA function and of the CVA VaR, and we show that some of the ad hoc assumptions used in practice by industry may result in a substantial misestimation of extreme CVA movements.

A Appendix: Numerical results

Table 7: Impact of λ_0 on the current CVA and on the 99% CVA VaR, over horizons of 10 days and 1 month for Bermudan put options. Other parameter values are given in Table 1.

		$S_0/K = 0.5$			$S_0/K = 1$			$S_0/K = 1.5$		
T	λ_0	Current	10 days	1 month	Current	10 days	1 month	Current	10 days	1 month
2	0.05	0.1073	0.0223	0.0428	0.2475	0.0299	0.0360	0.0298	0.0232	0.0419
	0.1	0.2058	0.0294	0.0508	0.3429	0.0418	0.0430	0.0386	0.0303	0.0539
	0.15	0.3038	0.0349	0.0564	0.4320	0.0491	0.0448	0.0470	0.0372	0.0647
3	0.05	0.1073	0.0223	0.0428	0.3858	0.0308	0.0400	0.0829	0.0437	0.0782
	0.1	0.2058	0.0294	0.0508	0.5042	0.0421	0.0488	0.1006	0.0541	0.0952
	0.15	0.3038	0.0349	0.0564	0.6177	0.0518	0.0536	0.1176	0.0639	0.1103
4	0.05	0.1073	0.0223	0.0428	0.5144	0.0298	0.0414	0.1508	0.0616	0.1094
	0.1	0.2058	0.0294	0.0508	0.6443	0.0395	0.0484	0.1762	0.0738	0.1289
	0.15	0.3038	0.0349	0.0564	0.7795	0.0476	0.0530	0.2004	0.0854	0.1462
5	0.05	0.1073	0.0223	0.0428	0.6286	0.0292	0.0425	0.2247	0.0761	0.1344
	0.1	0.2058	0.0294	0.0508	0.7659	0.0377	0.0479	0.2559	0.0892	0.1551
	0.15	0.3038	0.0349	0.0564	0.8976	0.0444	0.0508	0.2858	0.1017	0.1735

Table 8: Impact of ν on the current CVA and on the 99% CVA VaR, over horizons of 10 days and 1 month for Bermudan put options. Other parameter values are given in Table 1.

		$S_0/K = 0.5$			$S_0/K = 1$			$S_0/K = 1.5$		
T	ν	Current	10 days	1 month	Current	10 days	1 month	Current	10 days	1 month
2	0.1	0.2058	0.0294	0.0508	0.3429	0.0418	0.0430	0.0386	0.0303	0.0539
	0.2	0.2057	0.0531	0.0913	0.3408	0.0606	0.0768	0.0384	0.0308	0.0542
	0.3	0.2057	0.0793	0.1401	0.3376	0.0821	0.1161	0.0380	0.0309	0.0554
3	0.1	0.2058	0.0294	0.0508	0.5042	0.0421	0.0488	0.1006	0.0541	0.0952
	0.2	0.2057	0.0531	0.0913	0.5006	0.0680	0.0934	0.0999	0.0549	0.0958
	0.3	0.2057	0.0793	0.1401	0.4951	0.0947	0.1420	0.0989	0.0550	0.0979
4	0.1	0.2058	0.0294	0.0508	0.6443	0.0395	0.0484	0.1762	0.0738	0.1289
	0.2	0.2057	0.0531	0.0913	0.6403	0.0691	0.0996	0.1748	0.0748	0.1297
	0.3	0.2057	0.0793	0.1401	0.6333	0.0997	0.1541	0.1727	0.0749	0.1324
5	0.1	0.2058	0.0294	0.0508	0.7659	0.0377	0.0479	0.2559	0.0892	0.1551
	0.2	0.2057	0.0531	0.0913	0.7611	0.0697	0.1022	0.2539	0.0905	0.1562
	0.3	0.2057	0.0793	0.1401	0.7522	0.1026	0.1623	0.2507	0.0905	0.1592

Table 9: Impact of σ on the current CVA and on the 99% CVA VaR, over horizons of 10 days and 1 month for Bermudan put options. Other parameter values are given in Table 1.

		$S_0/K = 0.5$			$S_0/K = 1$			$S_0/K = 1.5$		
T	σ	Current	10 days	1 month	Current	10 days	1 month	Current	10 days	1 month
	0.2	0.2058	0.0294	0.0508	0.3429	0.0418	0.0430	0.0386	0.0303	0.0539
2	0.25	0.2058	0.0320	0.0549	0.4814	0.0583	0.0597	0.1075	0.0669	0.1157
	0.3	0.2058	0.0345	0.0601	0.6261	0.0765	0.0796	0.2070	0.1090	0.1785
	0.2	0.2058	0.0294	0.0508	0.5042	0.0421	0.0488	0.1006	0.0541	0.0952
3	0.25	0.2058	0.0320	0.0549	0.7240	0.0603	0.0682	0.2436	0.1039	0.1775
	0.3	0.2058	0.0345	0.0601	0.9511	0.0781	0.0883	0.4321	0.1549	0.2511
	0.2	0.2058	0.0294	0.0508	0.6443	0.0395	0.0484	0.1762	0.0738	0.1289
4	0.25	0.2058	0.0320	0.0549	0.9400	0.0577	0.0694	0.3978	0.1312	0.2226
	0.3	0.2058	0.0345	0.0601	1.2463	0.0743	0.0886	0.6767	0.1858	0.2990
	0.2	0.2058	0.0294	0.0508	0.7659	0.0377	0.0479	0.2559	0.0892	0.1551
5	0.25	0.2058	0.0320	0.0549	1.1319	0.0539	0.0681	0.5549	0.1510	0.2544
	0.3	0.2058	0.0345	0.0601	1.5116	0.0695	0.0865	0.9205	0.2061	0.3297

Table 10: Impact of μ on the 99% CVA VaR over horizons of 10 days and 1 month for Bermudan put options. Other parameter values are given in Table 1.

		$S_0/K = 0.5$		$S_0/K = 1$		$S_0/K = 1.5$	
T	μ	10 days	1 month	10 days	1 month	10 days	1 month
	0.05	0.0294	0.0508	0.0418	0.0430	0.0303	0.0539
2	0.075	0.0293	0.0504	0.0418	0.0420	0.0300	0.0524
	0.1	0.0289	0.0497	0.0412	0.0420	0.0297	0.0517
	0.05	0.0294	0.0508	0.0421	0.0488	0.0541	0.0952
3	0.075	0.0293	0.0504	0.0423	0.0477	0.0536	0.0928
	0.1	0.0289	0.0497	0.0416	0.0476	0.0530	0.0917
	0.05	0.0294	0.0508	0.0395	0.0484	0.0738	0.1289
4	0.075	0.0293	0.0504	0.0398	0.0481	0.0732	0.1260
	0.1	0.0289	0.0497	0.0391	0.0478	0.0723	0.1244
	0.05	0.0294	0.0508	0.0377	0.0479	0.0892	0.1551
5	0.075	0.0293	0.0504	0.0378	0.0476	0.0885	0.1519
	0.1	0.0289	0.0497	0.0373	0.0472	0.0874	0.1499

Table 11: Impact of $\theta^{\mathbb{P}}$ on the 99% CVA VaR over horizons of 10 days and 1 month for Bermudan put options. Other parameter values are given in Table 1.

		$S_0/K = 0.5$		$S_0/K = 1$		$S_0/K = 1.5$	
T	θ^P	10 days	1 month	10 days	1 month	10 days	1 month
	0.1	0.0294	0.0508	0.0418	0.0430	0.0303	0.0539
2	0.05	0.0263	0.0414	0.0390	0.0345	0.0298	0.0530
	0.15	0.0320	0.0589	0.0445	0.0503	0.0309	0.0547
	0.1	0.0294	0.0508	0.0421	0.0488	0.0541	0.0952
3	0.05	0.0263	0.0414	0.0385	0.0376	0.0531	0.0938
	0.15	0.0320	0.0589	0.0455	0.0586	0.0551	0.0966
	0.1	0.0294	0.0508	0.0395	0.0484	0.0738	0.1289
4	0.05	0.0263	0.0414	0.0354	0.0367	0.0725	0.1270
	0.15	0.0320	0.0589	0.0432	0.0594	0.0751	0.1308
	0.1	0.0294	0.0508	0.0377	0.0479	0.0892	0.1551
5	0.05	0.0263	0.0414	0.0334	0.0354	0.0877	0.1529
	0.15	0.0320	0.0589	0.0413	0.0590	0.0907	0.1574

Table 12: Impact of $\xi^{\mathbb{P}}$ on the 99% CVA VaR over horizons of 10 days and 1 month for Bermudan put options. Other parameter values are given in Table 1.

		$S_0/K = 0.5$		$S_0/K = 1$		$S_0/K = 1.5$	
T	ξ^P	10 days	1 month	10 days	1 month	10 days	1 month
2	1	0.0294	0.0508	0.0418	0.0430	0.0303	0.0539
	0.25	0.0297	0.0519	0.0420	0.0439	0.0301	0.0532
	1.75	0.0292	0.0499	0.0417	0.0421	0.0305	0.0534
3	1	0.0294	0.0508	0.0421	0.0488	0.0541	0.0952
	0.25	0.0297	0.0519	0.0424	0.0505	0.0537	0.0941
	1.75	0.0292	0.0499	0.0418	0.0477	0.0543	0.0946
4	1	0.0294	0.0508	0.0395	0.0484	0.0738	0.1289
	0.25	0.0297	0.0519	0.0400	0.0503	0.0732	0.1275
	1.75	0.0292	0.0499	0.0390	0.0476	0.0740	0.1283
5	1	0.0294	0.0508	0.0377	0.0479	0.0892	0.1551
	0.25	0.0297	0.0519	0.0382	0.0499	0.0886	0.1535
	1.75	0.0292	0.0499	0.0370	0.0467	0.0895	0.1544

Table 13: Impact of ρ and ν_λ on the current CVA and on the 99% CVA VaR, over horizons of 10 days and 1 month for interest rate payer swaps. Other parameter values are given in Table 6.

		$\rho = -0.5$			$\rho = 0$			$\rho = 0.5$		
T	ν_λ	Current	10 days	1 month	Current	10 days	1 month	Current	10 days	Current
2	0.1	6.39	5.20	8.60	7.16	5.79	9.93	7.97	6.48	11.22
	0.2	5.66	4.64	7.80	7.14	5.87	10.17	8.74	7.33	12.81
	0.3	4.93	4.20	7.00	7.05	6.02	10.57	9.47	8.13	14.42
3	0.1	13.07	7.89	13.46	14.72	8.76	15.44	16.45	9.82	17.38
	0.2	11.50	7.02	12.17	14.64	8.86	15.79	18.08	11.04	19.72
	0.3	9.84	6.27	10.77	14.36	9.03	16.19	19.52	12.18	22.07
4	0.1	20.39	9.91	17.13	23.00	10.94	19.54	25.73	12.24	21.88
	0.2	17.91	8.81	15.46	22.85	11.02	19.84	28.27	13.66	24.67
	0.3	15.11	7.81	13.57	22.22	11.18	20.21	30.35	15.01	27.39
5	0.1	27.62	11.28	19.67	31.14	12.39	22.37	34.84	13.84	24.91
	0.2	24.24	10.05	17.76	30.92	12.46	22.64	38.24	15.38	27.91
	0.3	20.21	8.84	15.48	29.81	12.57	22.88	40.80	16.80	30.76

References

[1] Basel Committee on Banking Supervision. (2006). Basel II: International Convergence of Capital Measurement and Capital Standards: A Revised Framework - Comprehensive Version. Bank for International Settlements.

[2] Basel Committee on Banking Supervision. (2011). Basel III: A Global Regulatory Framework for More Resilient Banks and Banking Systems. Bank for International Settlements.

[3] Breton, M. and Marzouk, O. (2018). Evaluation of Counterparty Risk for Derivatives with Early Exercise Features. GERAD working paper G-2015-62, forthcoming in the Journal of Economics Dynamic and Control.

[4] Brigo, D., Capponi, A., Pallavicini, A., and Papatheodorou, V. (2013). Pricing Counterparty Risk Including Collateralization, Netting Rules, Re-Hypothecation and Wrong-Way Risk. International Journal of Theoretical and Applied Finance. 6(2).

[5] Brigo, D., and Masetti, M. (2006). Risk Neutral Pricing of Counterparty Risk. In: Pykhtin, M. (Editor), Counterparty Credit Risk Modelling: Risk Management, Pricing and Regulation. Risk Books, London.

[6] Brigo, D., Morini, M., and Pallavicini, A. (2013). Counterparty Credit Risk, Collateral and Funding: With Pricing Cases For All Asset Classes. Wiley Finance.

[7] Cesari, G., Aquilina, J., Charpillon, N., Filipovic, Z., Lee, G., and Manda, I. (2009). Modelling, pricing, and hedging counterparty credit exposure: A technical guide. Springer Finance.

[8] Gregory, J. (2010). Counterparty credit risk: the new challenge for global financial markets (Vol. 470). John Wiley & Sons.

[9] Gregory, J. (2012). Counterparty Credit Risk and Credit Value Adjustment: A Continuing Challenge for Global Financial Markets. John Wiley and Sons.

[10] Pykhtin, M. (2012). Model foundations of the Basel III standardised CVA charge, Risk, July, pp. 60–66.